

Quantitative determination of many-body-induced interlayer charge transfer in bilayer electron systems via Shubnikov–de Haas measurements

X. Ying,* S. R. Parihar, H. C. Manoharan, and M. Shayegan

Department of Electrical Engineering, Princeton University, Princeton, New Jersey 08544

(Received 3 August 1995)

Direct determination of subband densities via measurements of Shubnikov–de Haas oscillations in coupled bilayer electron systems reveals a many-body-induced interlayer charge transfer as the front layer is depleted by a front-gate bias: with decreasing front-gate bias the back-layer electron density *increases* while the front-layer density decreases *faster than linearly*. The data are in excellent quantitative agreement with a self-consistent calculation that includes exchange and correlation energies via local-density approximation.

Coupled bilayer electron systems (BLES's) exhibit intriguing phenomena arising from Coulomb interaction and tunneling.^{1–3} Examples include the interlayer-interaction-driven destruction of certain integral quantum Hall states¹ or the creation of unique *even-denominator* fractional quantum Hall states² in the presence of a strong perpendicular magnetic field. Of particular relevance to the subject of this paper is the peculiar behavior of layer densities in an interacting BLES as one of the layers is depleted. Near the depletion of the front layer, transport measurements⁴ have revealed a sharp and significant change in the in-plane resistance of BLES's with appropriate parameters, suggesting an abrupt double- to single-layer transition driven by an exchange-enhanced charge-transfer instability. Compressibility⁵ data have also indicated that some charge is transferred from the front to the back layer as the front layer is being depleted.

Here we report a quantitative and direct determination of the interlayer charge transfer in BLES's via measurements of Shubnikov–de Haas (SdH) oscillations and a comparison of the data with the results of our self-consistent calculations. Our BLES's are confined in GaAs/Al_xGa_{1–x}As double-quantum-well samples, and we use a bias voltage (V_g) between a front gate and the BLES to deplete the electrons. The frequencies of the SdH oscillations directly give the electron densities of the occupied BLES electric subbands. These *subband* densities also represent the *layer* densities in the two wells when the BLES charge distribution is driven far from being symmetric for large $|V_g|$. Consistent with previous results,^{4,5} with decreasing V_g and near depletion of the front layer, the front-layer electron density shows a faster than linear decrease while the back-layer density *increases*, revealing that some charge transfer from the front layer to the back layer takes place in the depletion process. The data can be explained remarkably well by a self-consistent calculation which includes the exchange-correlation energies via a local-density approximation.⁶ Our measurements and calculations also reveal that the amount of charge transfer is only weakly dependent on interwell tunneling.

The samples were grown by molecular-beam epitaxy and each consists of two GaAs quantum wells of width W separated by an AlAs barrier of width d . The structure is cladded by undoped (spacer) and Si-doped layers of Al_xGa_{1–x}As barriers on both sides. The parameters W and d for the two

structures studied here are listed in Table I. Contacts (to both electron layers) were made by alloying In in a reducing atmosphere for about 10 min. The experiments were carried out in a pumped ³He system ($T \approx 0.5$ K), and the lock-in technique was used for the transport measurements. In Table I we list the measured total areal density N_{tot} and the low-temperature mobility μ for our BLES's when they contain a symmetric charge distribution in the double quantum well. Also listed are the subband energy separations, Δ_{SAS} .⁷

In our experiments, we measure the frequencies of the SdH oscillations. These frequencies f_i directly give the densities N_i of the populated electric subbands of the BLES: $N_i = (2e/h)f_i$.⁸ Before presenting the experimental data, it is useful to clarify the distinction between *layer* and *subband* densities in a coupled BLES. We confine ourselves to the case where at most two subbands are populated. For a “balanced” BLES, i.e., one with a symmetric total charge distribution in the double quantum well, the lowest two subbands correspond to the symmetric and antisymmetric states with Δ_{SAS} denoting their energy difference. Such a BLES is illustrated in Fig. 1 (top) where we show the results of our self-consistent calculations for the conduction-band-edge profile, the electron wave functions, and the charge distribution. This simulation is for sample A with $N_{\text{tot}} = 2.34 \times 10^{11} \text{ cm}^{-2}$. Note that the subband densities N_1 and N_2 are different because of the finite interlayer tunneling; their difference is equal to $(m^*/\pi\hbar^2)\Delta_{\text{SAS}}$, where m^* is the electron effective mass and $(m^*/\pi\hbar^2)$ is the two-dimensional density of states. In this case, of course, the front- and back-layer densities, N_f and N_b , are equal.⁹

In Fig. 1 (bottom) we present the results of simulations for the same structure, but here we assume a negative front-gate bias is employed to deplete a significant number of the front-layer electrons and to drive the BLES grossly out of balance. The energy difference between the lowest two subbands is now substantially larger than Δ_{SAS} as evidenced by

TABLE I. Parameters for the double-quantum-well samples.

Sample	d (Å)	W (Å)	N_{tot} (10^{11} cm^{-2})	μ ($10^6 \text{ cm}^2 \text{ V s}$)	Δ_{SAS} (K)
A (M229)	14	180	2.3	1.0	10
B (M293)	70	150	2.2	0.8	0.01

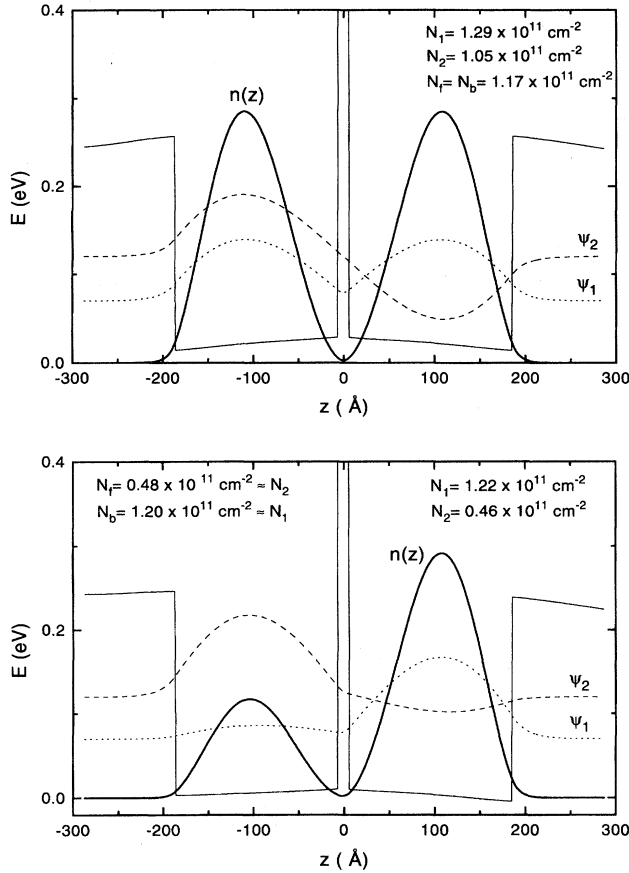


FIG. 1. Results of self-consistent calculations, performed in the local-density approximation, for a double quantum well (sample A). Shown here are the conduction-band-edge profile (thin solid curves), the charge distribution function $n(z)$ (thick solid curves), and the subband wave functions ψ_1 and ψ_2 . The calculated subband densities (N_1 and N_2) and the front- and back-layer densities (N_f and N_b) are also listed. The top figure corresponds to the “balanced” case where $N_f = N_b$ and the bottom one to the case where the system is grossly out of balance; note that in the latter case, the subband and layer densities are approximately equal: $N_1 \approx N_b$ and $N_2 \approx N_f$.

the much larger ($N_1 - N_2$) compared to the balanced case. Note also that here the layer densities are nearly equal to the subband densities: $N_b \approx N_1$ and $N_f \approx N_2$. The results of Fig. 1 illustrate a general property of the BLES: when the double quantum well is driven grossly out of balance so that the difference between the lowest subband energies becomes large compared to Δ_{SAS} , the electrons in the two subbands become localized in the individual wells and the subband densities become nearly equal to the layer densities.

In Fig. 2(a) we show the resistance (R) of sample A, measured as a function of the magnetic field (B) applied perpendicular to the sample plane. Figure 2(b) shows the Fourier-transform power spectra of the R vs B^{-1} data. At $V_g = -0.3$ V, only a single frequency oscillation is detected for $B \leq 0.5$ T.⁸ For $V_g = -0.2$ and -0.1 V, beating patterns appear in the SdH oscillations and the Fourier-transform spectra show two distinct frequencies, revealing that electrons now occupy two electric subbands. In Fig. 3 we plot

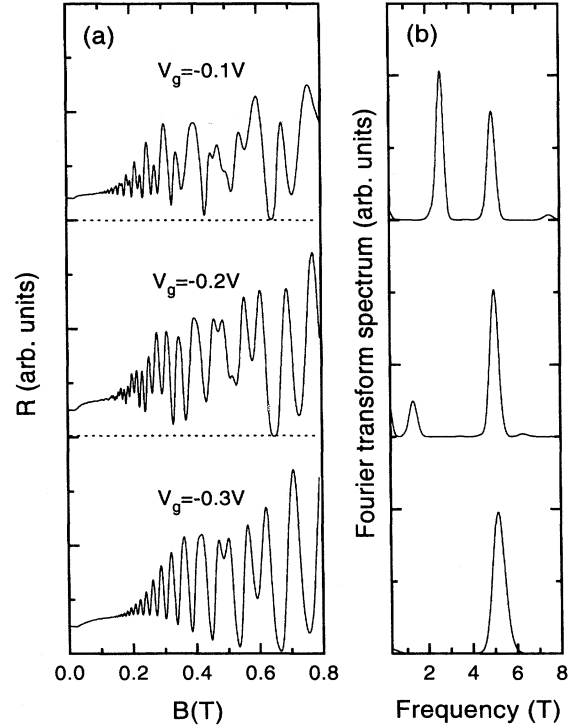


FIG. 2. Shubnikov-de Haas oscillations (left panel) and the corresponding Fourier-transform power spectra (right panel) of sample A for the indicated values of the front-gate voltage V_g .

these measured subband densities (filled symbols) as a function of V_g . At $V_g = 0.07$ V, the difference between subband densities (or, equivalently, subband energies) is a minimum and the BLES is balanced. For $V_g \leq -0.15$ V the bottom subband density which, as seen from Fig. 2(b), corresponds to the back-layer density, increases with decreasing V_g before finally decreasing for $V_g < -0.3$ V when the front layer is completely depleted. At the same time the front-layer density, which is nearly equal to the top subband density, shows a faster than linear decrease with decreasing V_g .

This anomalous charge transfer between the layers is not expected in a simple electrostatic picture of the BLES where the front layer screens the back layer by terminating the electric field induced by the gate bias. In fact, because of the imperfect screening by the front layer (since the density of states is finite), one would expect a slight decrease in the bottom layer density with decreasing V_g as the top layer is being depleted. In agreement with this expectation are the results of our Hartree calculations, performed by solving the Schrödinger and Poisson equations self-consistently. The calculated subband densities, shown by dashed curves in Fig. 3, match the measured values when the BLES is nearly balanced but are in clear disagreement with the data for $V_g \leq -0.15$ V.

The origin of the interlayer charge transfer is the dominance of the Coulomb energy over the kinetic energy in the front layer when this layer becomes nearly depleted.^{4,5} In order to quantitatively explain our data, many-body effects beyond the Hartree approximation must be considered. We incorporated the exchange and correlation energies in our

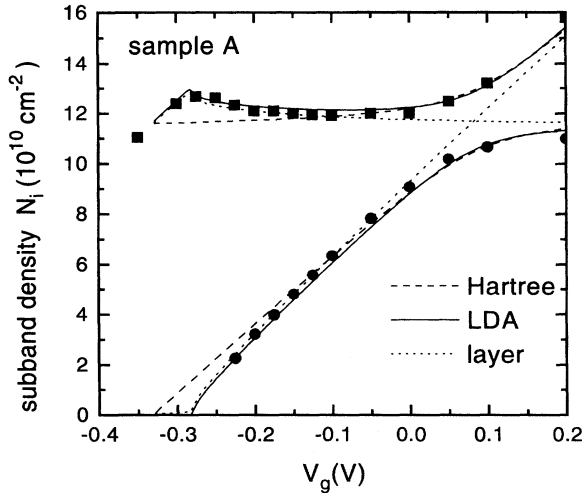


FIG. 3. The measured densities of the upper subband (circles) and lower subband (squares) of sample *A* are shown as a function of V_g . The solid curves are the subband densities from a (Hartree-Fock) self-consistent calculation which includes the exchange-correlation energy via a LDA, while the dashed curves are the subband densities calculated in a Hartree model where the exchange-correlation is ignored. The dotted curves are the layer densities deduced from the LDA calculation.

self-consistent calculations for the BLES's, by employing Hedin-Lundqvist's functional in a local-density approximation (LDA).⁶ In Fig. 3, the electron subband densities calculated in this model for sample *A* are shown by the solid curves. Note the excellent quantitative agreement between the experimentally measured and the calculated subband densities. The calculated layer densities are also shown in Fig. 3 (dotted curves). As expected (cf. Fig. 1), when the energy difference between the subbands is large compared to Δ_{SAS} (i.e., when $V_g \lesssim -0.15$ V), the subband densities correspond to the layer densities very closely.

The many-body-induced charge transfer is a direct consequence of the negative compressibility of a dilute two-dimensional electron system.⁵ The negative compressibility, which is a result of the dominance of the exchange-correlation energy at low densities, leads to a negative ratio of the differential penetration and external fields, $\delta E_p / \delta E_0$, where E_0 is the external electric field (induced by the front-gate bias) and E_p is the penetrating field that reaches the back layer. A negative compressibility means that δE_p has the opposite sign of δE_0 and therefore the back-layer density should increase as the front layer is being depleted by a negative gate bias. Our data and conclusions are quantitatively consistent with the results of Eisenstein, Pfeiffer, and West,⁵ who also found very good agreement between their data and a similar LDA calculation of the compressibility.

Since the charge transfer is a result of the Coulomb interaction, one would expect that interlayer tunneling should play a relatively minor role in determining the amount of charge transfer. Our results for sample *B*, shown in Fig. 4, confirm this expectation. The charge transfer for the two samples *A* and *B* is very similar, while tunneling (Δ_{SAS}) is about three orders of magnitude smaller in sample *B*. Note in

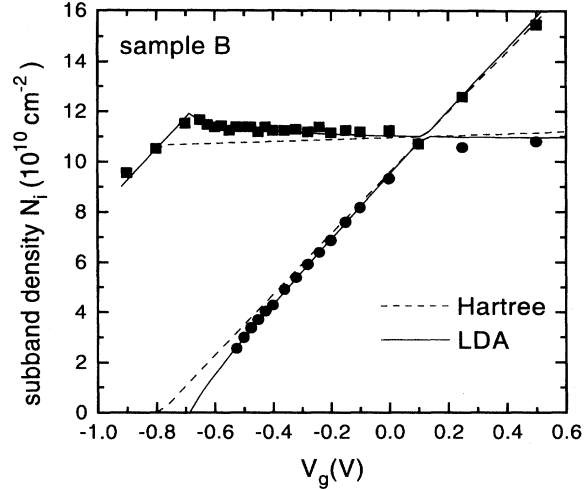


FIG. 4. Filled symbols are the measured subband densities of sample *B*. The solid (dashed) lines represent the calculated subband densities with (without) the exchange-correlation energy.

Fig. 4 that here again we find excellent agreement between the data and the LDA calculations. Note also that because Δ_{SAS} is quite small for sample *B*, the subband and layer densities are essentially equal for all values of V_g .¹⁰

Finally, we remark on the relative size of this interaction-induced interlayer charge transfer and the possibility that it may lead to an instability where the front-layer electrons would suddenly transfer to the back layer.^{4,11} For a very dilute system, such an instability was in fact suggested by Ruden and Wu,¹¹ based on consideration of the exchange energy in a simple model where the electrons are assumed to lie in sheets of zero thickness. In Fig. 5 we show the results of our self-consistent calculations for the structure of sample *B* for a very dilute case. It is clear that the relative amount of charge transfer (as a percentage of the total charge in the

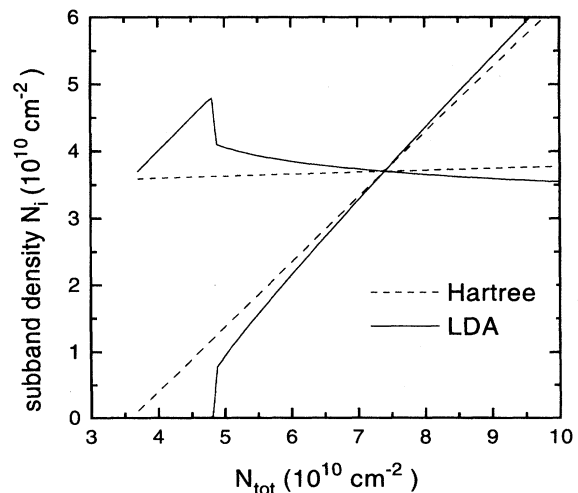


FIG. 5. Results of self-consistent calculations for the structure of sample *B* but assuming a much lower density than in Fig. 4. The LDA calculations predict a larger charge transfer than in Fig. 4 and a sudden layer density change near the front-layer depletion point.

wells) increases as the system becomes more dilute. Moreover, there is a sudden transfer of charge near the depletion of the front layer. We have not yet identified such a sudden charge transfer in SdH experiments.

In summary, we have presented SdH measurements of BLES subband densities which agree very well with the results of our self-consistent LDA calculations. In agreement with previous studies,^{4,5} the inclusion of the exchange-correlation energy in the calculations is essential, and ex-

plains the charge transfer from the front layer to the back layer as the former is depleted.

We thank M. B. Santos for the fabrication of sample *A* and J. P. Lu, S. Papadakis, T. S. Lay, and D. C. Tsui for many useful discussions. H.C.M. acknowledges financial support from the Fannie and John Hertz Foundation. This work was supported by the National Science Foundation and the Army Research Office.

*Present address: Intel Corporation, 5200 NE Elam Young Parkway, Hillsboro, OR 97124.

¹G. S. Boebinger, H. W. Jiang, L. N. Pfeiffer, and K. W. West, Phys. Rev. Lett. **64**, 1793 (1990); Y. W. Suen, J. Jo, M. B. Santos, L. W. Engel, S. W. Hwang, and M. Shayegan, Phys. Rev. B **44**, 5974 (1991).

²Y. W. Suen, L. W. Engel, M. B. Santos, M. Shayegan, and D. C. Tsui, Phys. Rev. Lett. **68**, 1379 (1992); J. P. Eisenstein, G. S. Boebinger, L. N. Pfeiffer, and S. He, *ibid.* **68**, 1383 (1992); Y. W. Suen, H. C. Manoharan, X. Ying, M. B. Santos, and M. Shayegan, *ibid.* **72**, 3405 (1994).

³J. P. Eisenstein, L. N. Pfeiffer, and K. W. West, Phys. Rev. Lett. **69**, 3804 (1992).

⁴Y. Katayama, D. C. Tsui, H. C. Manoharan, and M. Shayegan, Surf. Sci. **305**, 405 (1994); Y. Katayama, D. C. Tsui, H. C. Manoharan, S. Parihar, and M. Shayegan (unpublished).

⁵J. P. Eisenstein, L. N. Pfeiffer, and K. W. West, Phys. Rev. B **50**, 1760 (1994).

⁶L. Hedin and B. I. Lundqvist, J. Phys. C **4**, 2064 (1971); F. Stern and S. Das Sarma, Phys. Rev. B **30**, 840 (1984).

⁷In Table I, the measured Δ_{SAS} is listed for sample *A* while Δ_{SAS} for the other sample is too small to measure and the listed value is from our calculations. Also, for sample *A* we used a value of W which is 10% smaller than the nominal growth value (200 Å) so that the calculated Δ_{SAS} agrees with the measured Δ_{SAS} . Given the uncertainty in our growth parameters ($\approx \pm 15\%$), using $W=180$ Å is reasonable.

⁸We confine our analysis of the SdH data to very low magnetic fields (≤ 0.5 T) where spin splitting is not resolved.

⁹We define *layer density* as the integral of the charge distribution: $\int_0^{\pm\infty} n(z) dz$, where the $-$ sign is for N_f and the $+$ sign for N_b (Fig. 1).

¹⁰On the scale of Fig. 4, the calculated layer densities overlap with subband densities and are not shown for clarity.

¹¹P. P. Ruden and Z. Wu, Appl. Phys. Lett. **59**, 2165 (1991).